J. Membrane Biol. 94, 163–171 (1986)

The Journal of
Membrane Biology

A Kinetic Analysis of the Electrogenic Pump of *Chara corallina*: IV. Temperature Dependence of the Pump Activity

Nobunori Kami-ike, Taka-aki Ohkawa, Uichiro Kishimoto, and Yuko Takeuchi
Department of Biology, College of General Education, Osaka University, Toyonaka, 560 Japan

Summary. The sigmoidal current-voltage curve (i_p-V curve) of the electrogenic H^+-pump of the *Chara* membrane was simulated satisfactorily with a simple reaction kinetic model which assumed consecutive changes in state of H^+-ATPase. Four rate constants, i.e., forward and backward ones in voltage-dependent and -independent steps, could be evaluated from the data. The emf of the pump (E_p), the voltage at which the pump current changes its sign, varies only slightly with temperature. However, the pump current (i_p) is highly temperature dependent, and therefore the conductance (g_p) of the pump, calculated as the chord conductance from the i_p-V curve, is also highly voltage dependent having a peak at a level somewhat less negative than the resting potential. In contrast to g_p, the conductance (g_d) of the passive channel does not change appreciably with temperature. Arrhenius plots of g_p and also of the rate constants showed a clear bend at about 19°C. Great temperature dependence of the kinetic parameters offers useful information on the pumping mechanism of the *Chara* membrane.

Key Words *Chara* · electrogenic pump · I-V curve · chord conductance · kinetic model · temperature dependence

Introduction

The influence of temperature on membrane potential and conductance has been studied by Hogg, Williams and Johnson (1968) with *Nitella* and by Hope and Aschberger (1970) with *Chara* and *Griffithsia*. Arrhenius plots of the permeabilities of the plasmalemma of these cells calculated from electrical data gave single lines between 5 and 20°C. On the other hand, similar plots calculated from influxes of K^+ or Na^+ were nonlinear. Kishimoto (1972) showed that in *Chara* the transient current and the steady-state current under the voltage clamp are highly temperature dependent. Blatt (1974) showed in *Nitella flexilis* the presence of a relatively sharp discontinuity at about 13.5°C in the slope of the Arrhenius plot of the rise and decay times of the action potential. Beilby and Coster (1979) also found that in *Chara corallina* the transient current under the voltage clamp is highly temperature dependent. They showed that Arrhenius plots of the inverse of the activation and inactivation time constants and also of the delay time for the onset of activations of the Cl^- channel and possibly of the Ca^{2+} channel were almost linear between 4 and 30°C. They gave 60 kJ/mol for the activation enthalpy and 40 kJ/mol for the inactivation enthalpy, which were independent of the membrane potential. Such studies on the temperature dependence of the electrical characteristics of *Chara* membranes were carried out without separating the active ion transport process from the passive one.

The electrogenic H^+-pump appears to be the primary active transport system in green algae (*see* review by Spanswick, 1981). We characterized the electrogenic pump with an electromotive force E_p having a conductance g_p in series (Kishimoto, Kami-ike & Takeuchi, 1980, 1981). This transport system coexists in the plasmalemma of characean internodes with the passive diffusion channels. Generally, the conductance of living membranes is highly dependent on changes in temperature, light and metabolic conditions. Therefore, it is of importance to study the extent of the contribution of the pump mechanism to the measured conductance.

The i_p-V curve of the electrogenic pump of the *Chara* membrane is normally sigmoidal and can be simulated successfully with a model which assumes consecutive changes of the state of H^+-ATPase. The kinetic parameters in this model can be evaluated with the aid of computer simulation of the experimental i_p-V curve (Kishimoto et al., 1984, 1985; Takeuchi et al., 1985). This method was used here to analyze the change in activity of the electrogenic H^+-pump with temperature.

Materials and Methods

Giant internodes of *Chara corallina* were used. Internodes, which averaged 0.7 mm in diameter and 6 cm in length, were

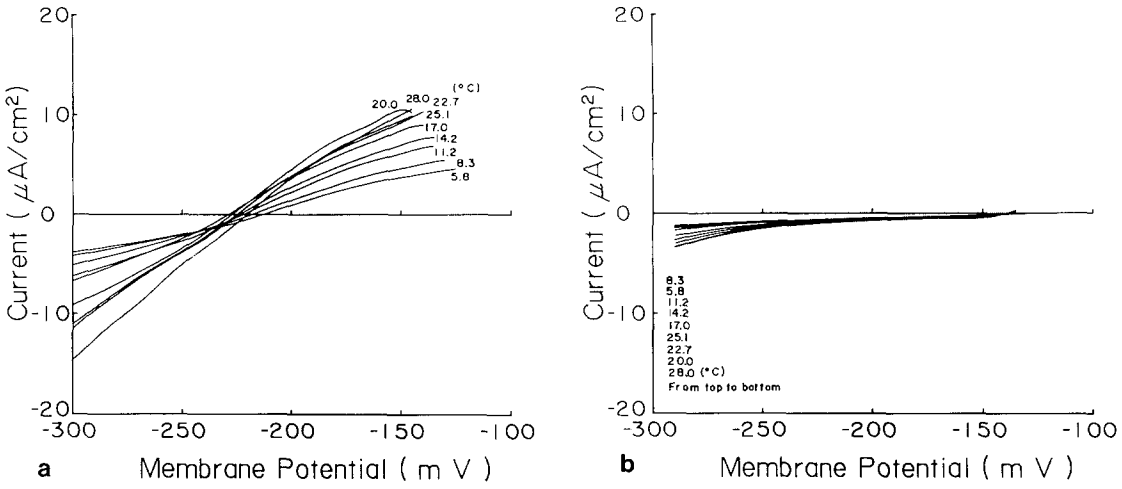

Fig. 1. (*a*) Changes of the *I-V* curve of the normal *Chara* membrane with temperature. (*b*) Changes of i_d-*V* curve of the passive diffusion channel with temperature. The latter curves were obtained after inhibiting the H^+-pump with 50 μM DCCD in the dark

isolated from adjacent cells and kept in artificial pond water (APW) for at least two days with a photo period of 12-hr light (ca. 2000 lx) and 12-hr dark. The APW, containing (in mM) 0.05 KCl, 0.2 NaCl, 0.1 $Ca(NO_3)_2$ and 0.1 $Mg(NO_3)_2$, was buffered at pH 7.0 with 2 mM TES (N-tris(hydroxylmethyl)methyl-2-amino-ethane sulfonic acid). APW was perfused at a constant rate of about 1 liter/hr. The temperature of the solution was controlled between about 6 to 30°C with a thermoelectric regulator (Sharp TE12K) and monitored with a thermistor. The external pH was monitored with a glass pH electrode.

The current-voltage curve (*I-V* curve) was obtained by applying a slow ramp hyperpolarization first then a slow ramp depolarization under the voltage-clamp condition. A steady state *I-V* relation could be attained when the ramp rate was as slow as 100 mV/30 sec (Kishimoto et al., 1984). This method gave one set of *I-V* curves within about 1 min and also enabled us to collect far more data points (>100) than when using the step voltage-clamp method. This is another merit of performing satisfactory simulation of the i_p-*V* curve of the electrogenic pump.

A set of *I-V* curves at different temperatures was obtained on a single internodal cell in the light (about 3000 lx) before inhibition of the pump. Temperature was lowered successively from 20 to 5.8°C (20 → 17 → 14.2 → 11.2 → 8.3 → 5.8°C) and then brought back to 20°C. The cell was left to stand for 5 to 10 min each time before reaching a steady state following temperature changes. Next, the temperature was elevated to about 28°C (20 → 22.7 → 25.1 → 28°C) and then brought back to 20°C.

Results

Temperature range was limited to between about 6 and 28°C, as the temperature below 5 and above 30°C caused some qualitative changes that lasted long after returning to the initial 20°C. Even in the temperature range between 5.8 and 28°C a hysteresis was observed frequently in the record of *I-V* curve, unless enough time was allowed for the cells to attain a new steady state. Below we present the one of the typical data for the single internodes in which the reversibility of the *I-V* curve were satisfactory.

Changes of *I-V* Curves with Temperature

Figure 1*a* shows the *I-V* curves of a single internode at different temperatures. After a series of experiments at different temperatures the same *Chara* internode was treated with 50 μM DCCD in the dark. At about 2 hr after application of DCCD, the pump activity is almost completely lost, while the passive channel remains active (Kishimoto et al., 1981, 1984, 1985; Takeuchi et al., 1985). Since the *I-V* curve at this steady state is presumed to be the i_d-*V* curve of the passive diffusion channel, a second series of i_d-*V* curves was obtained in the same temperature range (Fig. 1*b*). In contrast to the *I-V* curves, the i_d-*V* curve showed little temperature dependence.

Changes of i_p-*V* Curve with Temperature

Since the *I-V* curve and the i_d-*V* curve of the passive channel are known at each temperature, the i_p-*V* curve of the electrogenic pump channel can be obtained by subtracting the latter from the former (Kishimoto et al., 1981, 1984, 1985; Takeuchi et al., 1985). The i_p-*V* curves in the temperature range between 5.8 and 28°C are shown in Fig. 2. The symbols in this figure are the experimental data plotted at 5-mV intervals. The solid lines are the simulated i_p-*V* curves [Eq. (A3)]. The result of simulation assuming the consecutive change of H^+-ATPase at the plasmalemma of the *Chara* was satisfactory in

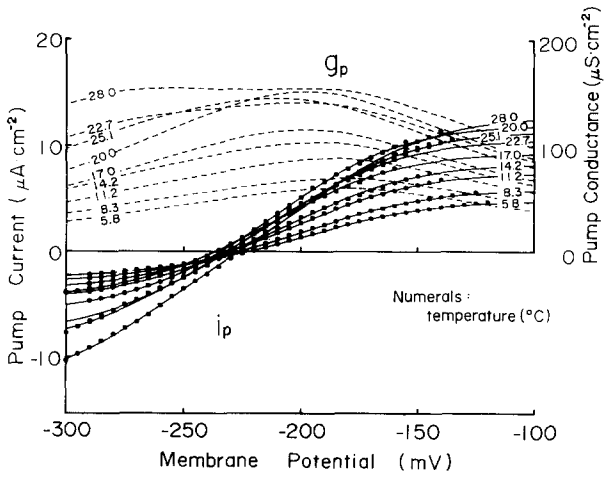

Fig. 2. Changes of i_p-V curve of the electrogenic H^+-pump with temperature. The i_p-V curves were obtained by subtracting the i_d-V curve (Fig. 1*b*) of the passive channel from the I-V curve (Fig. 1*a*) at the respective temperature. The symbols are the experimental data plotted for 5-mV intervals. Solid lines are the results of simulation with Eq. (A3). Dotted lines are the chord conductance calculated from the i_p-V curve with Eq. (A9). Note that the i_p-V curve and also the g_p-V curve became markedly suppressed by lowering of the temperature, while depolarization of E_p (reversal potential for the pump) was only slight

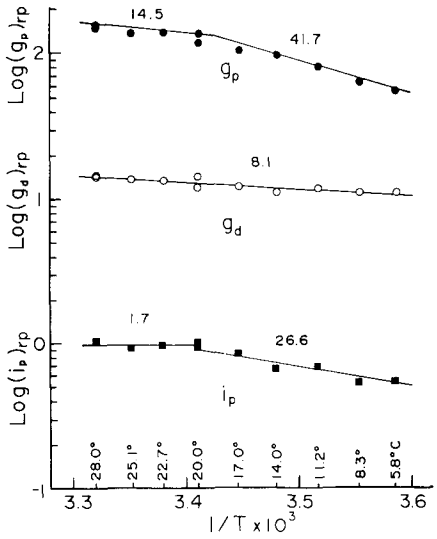

Fig. 3. Logarithms of conductance (g_p), current (i_p) of the pump channel, and conductance (g_d) of the passive channel at the resting potential (rp) in relation to the reciprocal of temperature. These Arrhenius plots of g_p (μS cm^{-2}) and i_p (μA cm^{-2}) consist of two lines of different slopes, which show discontinuities at around 19°C. In contrast, the Arrhenius plot of g_d does not show any appreciable bend

this temperature range and at an external pH of around 7. The dotted lines in Fig. 2 show the chord conductance of the pump calculated from the i_p-V curve [Eq. (A9)]. Note that the pump current and the chord conductance are highly temperature dependent, while the emf (E_p) of the pump is not.

Changes of Conductances and Pump Current with Temperature

Conductances of the electrogenic pump channel $(g_p)_{rp}$ and of the passive channel $(g_d)_{rp}$ as well as the pump current $(i_p)_{rp}$ at the resting membrane potential are plotted as logarithmic values against the reciprocal of temperature in Fig. 3. These Arrhenius plots of g_p and i_p generally gave two sets of lines showing discontinuities at around 19°C. This indicates that the pumping mechanisms differ below and above 19°C in the *Chara* membrane. Such a bend of line was almost nonexisting in the Arrhenius plot for g_d of the passive channel. Also the slope was not as large as that for g_p.

Changes of Pump Rate Constants with Temperature

Four forward rate constant, i.e., forward (k^o_{12}), backward (k^o_{12}) in the electrogenic step and forward (κ_{21}) and backward (κ_{12}) in the nonelectrogenic step could be calculated from A_1, A_2, A_3, A_4 and z. All of these were determined from the simulation of the experimental i_p-V curve (Kishimoto et al., 1984, 1985; Appendix, this paper). Since z was found to be very close to 2 in the *Chara* under the normal physiological condition, i.e., around neutral pH and under normal light, $z = 2$ in our computation for convenience. The forward and backward rate constants in the electrogenic step were assumed to be functions of voltage [Eqs. (A1) and (A2)]. The logarithms of these rate constants were plotted against the reciprocal of temperature in Fig. 4*a* at different membrane potentials. These Arrhenius plots consist of two sets of lines which show clear discontinuities around 19°C (Fig. 4*a*). A similar Arrhenius plot for κ_{21} in the nonelectrogenic step also had a bend at around 19°C, while that for κ_{12} was not appreciably large (Fig. 4*b*). These bends again indicate that the functional mode of the pump below 19°C differs from that above 19°C.

The slope of the line in the Arrhenius plot of each rate constant was determined by a linear regression method. The slope gives the heat of activation (E_A) in its respective direction. The E_A for the two rate constants in the electrogenic step is voltage dependent, while that in the nonelectrogenic step is voltage independent. In our model, E_A in the electrogenic step is shown explicitly by Eq. (1).

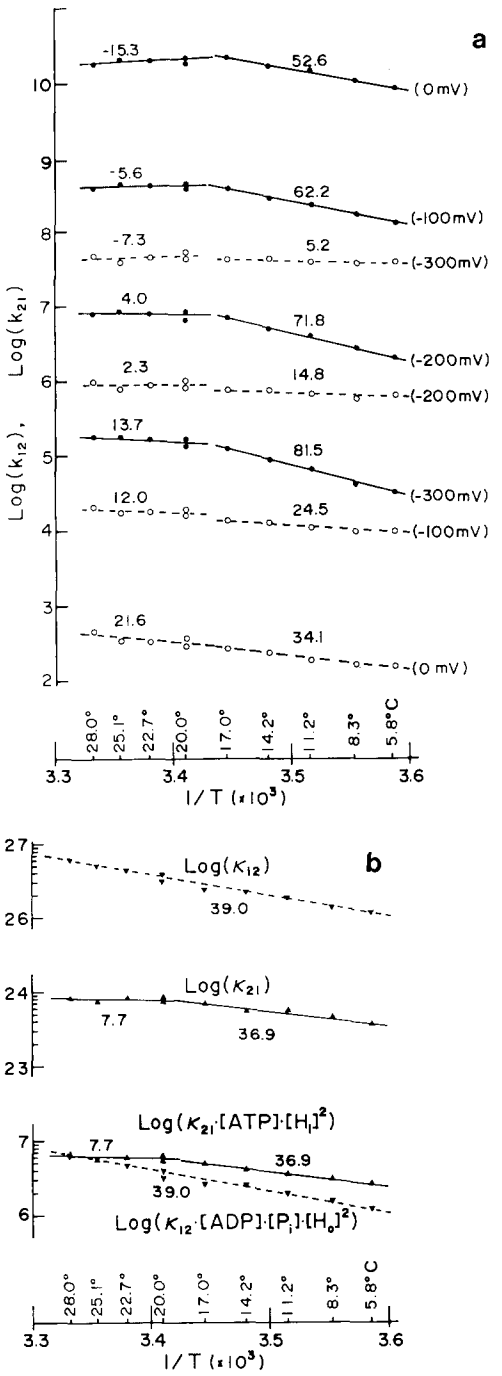

Fig. 4. (*a*) Arrhenius plots of rate constants, k_{12} and k_{21} in the electrogenic transition. Note that k_{12} at $V = 0$ mV is of the order of 10^{10} sec^{-1}, but decreases to the order of 10^6 or 10^7 sec^{-1} at $V = -200$ mV. On the other hand, k_{21} at $V = 0$ mV is of the order of 10^2 sec^{-1}, but increases to the order of 10^6 sec^{-1} at $V = -200$ mV. The slopes of $\ln(k_{12})$ and $\ln(k_{21})$ change not only with temperature, but also with voltage. (*b*) Arrhenius plots or rate constants, i.e., κ_{21} and κ_{12} in the nonelectrogenic transition. Note that κ_{21} is of the order of 10^{23} to 10^{24} mol^3 liter^{-3} sec^{-1}, while κ_{12} is of the order of 10^{26} mol^4 liter^{-4} sec^{-1}. These values do not change with voltage and change differently with temperature. Note that κ_{21} [ATP][H_i]^2 and κ_{12}[ADP][P_i][H_o]^2 are of the order of 10^6 to 10^7 sec^{-1}, which are of the same order as those of k_{12} and k_{21} at the resting potential (= −230 mV). Numerals near the curves give the heat of activation in kJ/mol calculated using Eqs. (1) and (2)

$$(E_A)_{12} = -R\partial \ln k_{12}/\partial(1/T) = -R\partial \ln k^o_{12}/\partial(1/T) - zFV/2 \quad (1)$$

and

$$(E_A)_{21} = -R\partial \ln k_{21}/\partial(1/T) = -R\partial \ln k^o_{21}/\partial(1/T) + zFV/2. \quad (2)$$

Note that the sign for the voltage dependence of $(E_A)_{12}$ is the opposite of that of $(E_A)_{21}$.

Changes of Enthalpy, Free Energy and Entropy in the Electrogenic Step and in the Nonelectrogenic Step

The change in enthalpy (ΔH_{ij}) for the transition from E_i to E_j is calculated as the difference of activation energies for the forward and backward transitions in each step. Changes in free energy and entropy in the electrogenic step and those in the nonelectrogenic step can be calculated as follows.

In the electrogenic step the change in free energy ΔG_{12} is,

$$\Delta G_{12} = \mu^o_2 - \mu^o_1 - RT \ln(k^o_{12}/k^o_{21}) + RT \ln(E_2/E_1) - zFV.$$

At equilibrium

$$0 = \mu^o_2 - \mu^o_1 - RT \ln(k^o_{12}/k^o_{21}) + RT \ln(E_2/E_1)_{Ep} - zFE_p.$$

Therefore,

$$\Delta G_{12} = zF(E_p - V) + RT[\ln(E_2/E_1) - \ln(E_2/E_1)_{Ep}]. \quad (3)$$

Note that ΔG_{12} in the electrogenic step depends not only directly, but also indirectly on the membrane potential, since the fractions of the enzyme state (E_2 and E_1) are voltage dependent. Also note that ΔG_{12} is zero when the membrane potential is equal to E_p.

On the other hand, the free energy change in the nonelectrogenic step is calculated as follows:

$$\Delta G_{21} = \mu^o_1 - \mu^o_2 - RT \ln(\kappa_{21}/\kappa_{12}) + RT \ln(E_1/E_2).$$

At equilibrium

$$0 = \mu^o_1 - \mu^o_2 - RT \ln(\kappa_{21}/\kappa_{12}) + RT \ln(E_1/E_2)_{Ep}.$$

Therefore,

$$\Delta G_{21} = RT[\ln(E_1/E_2) - \ln(E_1/E_2)_{Ep}]. \quad (4)$$

ΔG_{21} in the nonelectrogenic step is also voltage dependent, since E_1/E_2 depends on the membrane potential. ΔG_{21} is zero, when the membrane potential is equal to E_p.

Since ΔH_{ij} and ΔG_{ij} are known, the entropy change ΔS_{ij} is calculated as follows:

$$\Delta S_{ij} = (\Delta H_{ij} - \Delta G_{ij})/T. \quad (5)$$

Note that ΔS_{ij} is voltage dependent, since both ΔH_{ij} and ΔG_{ij} are voltage dependent as described above.

ΔH_{ij}, ΔG_{ij} and ΔS_{ij} during the electrogenic transition and during the nonelectrogenic transition in the kinetic model are shown in Fig. 5. Changes of these thermodynamical characteristic functions during the transition from E_1 to E_2 (electrogenic) and from E_2 to E_1 (nonelectrogenic) in the lower temperature range differ qualitatively from those in the higher temperature range.

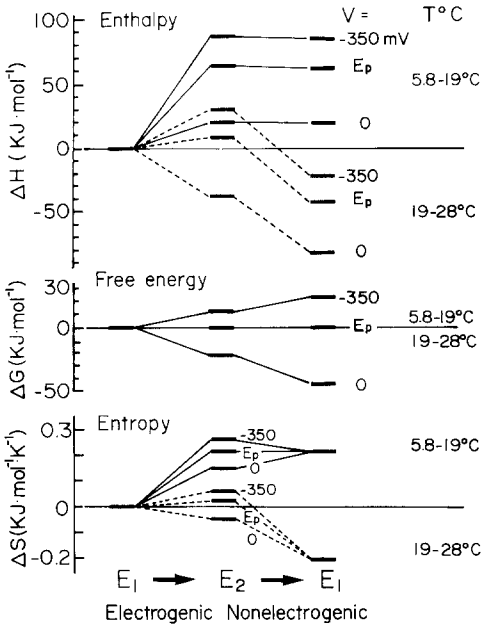

Fig. 5. Changes in enthalpy (ΔH_{12}), free energy (ΔG_{12}) and entropy (ΔS_{12}) for the forward transition in the electrogenic step ($E_1 \rightarrow E_2$) and ΔH_{21}, ΔG_{21} and ΔS_{21} in the nonelectrogenic transition from E_2 to E_1. Solid lines are those in the lower temperature range (5.8 ~ 19°C), while dotted lines in the higher temperature range (19° ~ 28°C). Plots are for three different membrane potentials, i.e., −350 mV, E_p and 0 mV

Discussion

Numerous biochemical data on the kinetic schemes of transport ATPases such as Na,K-ATPase, Ca-ATPase, and H^+-ATPase have been accumulated, mainly in animal cells (*see* Carafoli & Scarpa, 1982; Beaugé, 1984). Thermodynamics of Ca^{2+}-ATPase have been discussed (Inesi, 1985). All of these transport systems are supposed to be electrogenic. Nevertheless, it seems one seldom finds analyses based on their voltage dependence.

The emf or the reversal potential of the electrogenic H^+ pump of the *Chara* membrane depends not only on the adenine nucleotide levels ([ATP], [ADP] and [P_i]), but also on the ratio of external to internal H^+ concentration as well as on the rate constants in the kinetic model [Eq. (A8)]. The force which drives the proton is V-E_p in our circuit model (Fig. A1) and the pump current (i_p) is proportional to this driving force. The proportionality coefficient or the efficiency of the pumping mechanism is expressed with the chord conductance, i.e., g_p ($=i_p/(V-E_p)$) in our model [Eq. (A9)]. This is directly proportional to i_p and highly dependent on voltage and on temperature, whereas E_p itself changes only slightly with temperature (Fig. 2). In our kinetic analysis the i_p approaches $zFE_o\ \kappa_{21}[\mathrm{ATP}][H_i]^2$ for a large depolarization and approaches $-zFE_o\ \kappa_{12}[\mathrm{ADP}][P_i][H_o]^2$ for a large hyperpolarization [Eq. (A3)]. In other words, the magnitude of i_p depends directly on the rate constants in the nonelectrogenic transition, which are highly temperature dependent. Consequently, g_p is highly temperature dependent (Figs. 2 and 3). On the other hand, the ratios of the rate constants, i.e., k^o_{21}/k^o_{12} and κ_{21}/κ_{12}, change twice at most in this temperature range. The first and second terms in the expression for the E_p [Eq. (A8)] are logarithms of these two ratios, thus contributing little in the change in E_p with temperature. Note that the sum, i.e., $RT[\ln(k^o_{21}/k^o_{12}) + \ln(\kappa_{12}/\kappa_{21})]$ is about −30 kJ/mol (= −7.16 kcal/mol), which is comparable to the standard Gibbs free energy for the hydrolysis of ATP reported by Rosing and Slater (1972), and is also slightly temperature dependent. These results indicate that a kinetic reaction of the H^+-ATPase such as as shown in Fig. A2 (Appendix) is involved in the active proton extrusion.

The existence of H^+-pump activity in the *Nitella* membrane was first demonstrated by Kitasato (1968). The H^+-pump of the *Chara* membrane is supposed to be a Mg^{2+}-dependent ATPase (Shimmen & Tazawa, 1977), which seems to be blocked by internally applied vanadate (Shimmen & Tazawa, 1982). The activity of the pump is suppressed (depolarization and decrease of conductance of the membrane) by 5 μM CCCP, 100 μM DNP, or 40 μM DES (Keifer & Spanswick, 1978, 1979), and also by 5 μM triphenyltin chloride or 70 μM DCCD (Kishimoto et al., 1980, 1981, 1984). Internally applied EGTA ($[Ca^{2+}]_i < 1$ μM) was found to suppress the pump activity to a large extent (*unpublished*). These inhibitors probably attack the internal organelles including mitochondria and chloroplasts, reducing the internal ATP concentration. These inhibitors certainly reduce the internal ATP level of the *Chara* internode, but by half at most (Takeuchi & Kishimoto, 1983). The extent of the expected depolarization of E_p [the third term in Eq. (A8)] is less than 50 mV. Nevertheless, the decrease of g_p during inhibition was quite marked. This indicates that DCCD directly attacks the H^+ pump of the plasmalemma. We found that the internal ATP level did not change significantly within 1 hr for the change in

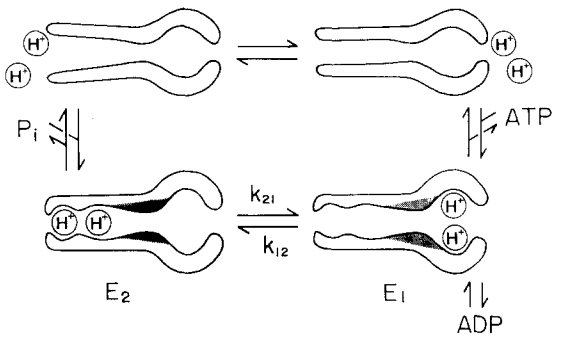

Fig. 6. A hypothetical scheme for the H^+ pump of the *Chara* membrane. *See* text for details

light condition (from 3000 to 0 1x, Takeuchi & Kishimoto, 1983), whereas the i_p-V curve as well as the g_p-V curve were markedly suppressed (*unpublished*). A sharp dependence of g_p on the internal ATP level may exist (Spanswick, 1980), but a more likely reason is that these inhibitors or light directly affect the kinetic process (Kishimoto et al., 1984).

Recently Sanders (1980) and Sanders and Hansen (1981) suggested the existence of electrogenic $2H^+/Cl^-$ cotransport system in *Chara corallina*. However, the possible current estimated from their data is one or two orders less than the one we recorded. Also we can suppose the existence of electrogenic Ca^{2+} pump. However, its contribution should be even much less judging from the extent of its flux. If some unidentified electrogenic systems other than H^+ pump were contributing appreciably to our current record, the i_p-V curve would deviate considerably from what Eq. (A3) presumes. This has not occurred, and thus we conclude that H^+-pump is a major electrogenic system in the *Chara* membrane under our normal experimental condition. However, under some other physiological conditions such as extreme change in pH or great voltage change our simple H^+-pump model does not necessarily fit the data.

Biochemical findings are not presently available for the H^+-pump of the *Chara* membrane to decide whether it is an E_1, E_2 type or a F_o, F_1 type. However, we do know that its function can be mimicked by the kinetic model (Figs. 6 and A2) which assumes consecutive changes of the state of H^+-ATPase. On the assumption that only a single step shown with two rate constants, i.e., k_{12} and k_{21}, is charge carrying and thus electrogenic, and that, for simplicity, binding and occlusion to and release from the H^+-ATPase of ATP, ADP, P_i and H^+ do not depend on the membrane potential, quite a satisfactory simulation was obtained for the experimental sigmoidal i_p-V curve of the *Chara* membrane. In another kinetic model where the transition shown with κ_{21} and κ_{12} is also electrogenic, the anticipated i_p-V curve deviates from the sigmoidal type and does not fit the experimental i_p-V curve.

The kinetic behavior described in this report may be visualized as the hypothetical change of H^+-ATPase as shown in Fig. 6. Binding of ATP induces a structure change in the enzyme, resulting in proton occlusion in its selective sites. The occluded protons need to be translocated across the enzyme structure to be released outside. Electrogenic transition of the enzyme state from E_1 to E_2 is expressed in the present analysis with two voltage dependent rate constants, i.e., k_{12} ($=k^o_{12}\exp(zFV/2RT)$) and k_{21} ($=k^o_{21}\exp(-zFV/2RT)$). When the membrane potial is zero, the forward rate constant k^o_{12} for the electrogenic transition is about eight orders of magnitude greater than the backward rate constant k^o_{21} (top and bottom curves in Fig. 4*a*). On the other hand, the forward rate constant κ_{21} for the nonelectrogenic transition is about three orders of magnitude less than the backward one κ_{12} (upper two curves in Fig. 4*b*). However, at the normal resting potential level (−230 mV) k_{12} is much smaller and k_{21} is much greater than those at 0 mV. These are almost of the same order at the normal resting potential level (Fig. 4*a*). It is of interest that $\kappa_{21}[ATP][H_i]^2$ and $\kappa_{12}[ADP][P_i][H_o]^2$ are also of the same order as k_{12} and k_{12} at the resting potential level, although they display different temperature dependence (Fig. 4*b*).

The heat of activation and also change in enthalpy for the electrogenic transition are voltage-dependent as described earlier [Eqs. (1) and (2)]. At lower temperature the enthalpy change for the forward electrogenic transition is 52.6 kJ/mol and for the backward transition is 34.1 kJ/mol, when the membrane potential is zero. However, the former rises to 71.8 kJ/mol, while the latter falls to 14.8 kJ/mol, when the membrane potential is −200 mV, which is close to the resting potential level (Fig. 4*a*). On the other hand, ΔG_{ij} is voltage dependent and equals zero, if the membrane potential is equal to E_p [Eqs. (3) and (4)]. Following these changes a large increase of entropy is expected for the electrogenic forward transition. These results indicate the presence of an endothermic and entropy-producing structural change in the enzyme during the electrogenic forward transition at lower temperature. Furthermore, the extent of these changes at the resting membrane potential is much greater than that at zero membrane potential. This change in structure possibly in a channel portion in the enzyme enables the occluded protons near the internal surface of the enzyme to be translocated to near the external surface before their release. On the other hand, the forward rate constant (κ_{21}) in the nonelectrogenic step is about three orders of magnitude less than the backward one (κ_{12}) at lower temperature. However,

the heat of activation for the forward transition (36.9 kJ/mol) is only slightly less than that for the backward one (39.0 kJ/mol, Fig. 4*b*). Consequently, the forward nonelectrogenic transition from E_2 to E_1 at lower temperature is slightly exothermic and the extent of the entropy change is not appreciable.

At higher temperature, however, the mechanism in these changes qualitatively differ from those at lower temperature. At higher temperature the enthalpy change for the electrogenic forward transition is 4.0 kJ/mol and that for the backward one is 2.3 kJ/mol, when the membrane potential is −200 mV (Fig. 4*a*). These are considerably less than those at lower temperature. Thermal fluctuation may assist the electrogenic forward transition at higher temperature. The forward electrogenic transition is endothermic for the more negative membrane potential but exothermic for the less negative membrane potential. The extent of the free energy change, ΔG_{ij}, is voltage dependent as described above and equals zero, when the membrane potential is equal to E_p. Accordingly, the entropy change is slight at the resting membrane potential, positive for the more negative potential, and negative for the less negative potential. On the other hand, the heat of activation for the nonelectrogenic forward transition (8.3 kJ/mol) is considerably less than that for the backward transition (39.0 kJ/mol) at higher temperature (Fig. 4*b*). Consequently, the nonelectrogenic transition from E_2 to E_1 is markedly exothermic and entropy consuming in the higher temperature range. The enzyme probably has a special restoring force in its structure to prevent from becoming a leaky channel, especially at higher temperature where thermal fluctuations around the enzyme are large.

In summary, the whole cycle of the electrogenic pump in the *Chara* membrane is endothermic and entropy producing at lower temperature, and free energy decreases slightly around the resting membrane potential level. On the other hand, the whole cycle is exothermic and entropy consuming at higher temperature. Here also the free energy decreases slightly around the resting membrane potential level.

We would like to thank Mr. Izuo Tsutsui for his technical assistance. We are indebted to Ms. Y. Saegusa for her excellent secretarial assistance. This work was supported by a Research Grant from the Ministry of Education, Science and Culture of Japan.

References

Beaugé, L. 1984. Sodium pump in squid axons. *Curr. Top. Membr. Transp.* **22**:131–175

Beilby, M.J., Coster, H.G.L. 1979. The action potential in *Chara corallina*. IV. Activation enthalpy of the Hodgkin-Huxley gates. *Aust. J. Plant. Physiol.* **6**:355–365

Blatt, F.J. 1974. Temperature dependence of the action potential in *Nitella flexilis*. *Biochim. Biophys. Acta* **339**:382–389

Carafoli, E., Scarpa, A. (editors). 1982. Transport ATPases. Vol. 402. *Ann. N. Y. Acad. Sci.* New York Academy of Sciences, New York

Chapman, J.B., Johnson, E.A., Kootsey, J.M. 1983. Electrical and biochemical properties of an enzyme model of the sodium pump. *J. Membrane Biol.* **74**:139–153

Hansen, U.-P., Gradmann, D., Sanders, D., Slayman, C.L. 1981. Interpretation of current-voltage relationships for "active" ion transport systems: I. Steady-state reaction-kinetic analysis of class-I mechanisms. *J. Membrane Biol.* **63**:165–190

Hogg, J., Williams, E.J., Johnson, R.J. 1968. The temperature dependence of the membrane potential and resistance in *Nitella translucens*. *Biochim. Biophys. Acta* **150**:640–648

Hope, A.B., Aschberger, P.A. 1970. Effects of temperature on membrane permeability to ions. *Aust. J. Biol. Sci.* **23**:1047–1060

Inesi, G. 1985. Mechanism of calcium transport. *Annu. Rev. Physiol.* **47**:573–601

Keifer, D.W., Spanswick, R.W. 1978. Activity of the electrogenic pump in *Chara corallina* as inferred from measurements of the membrane potential, conductance, and potassium permeability. *Plant Physiol.* **62**:653–661

Keifer, D.W., Spanswick, R.W. 1979. Correlation of adenosine triphosphate levels in *Chara corallina* with the activity of the electrogenic pump. *Plant Physiol.* **64**:165–168

Kishimoto, U. 1972. Characteristics of the excitable *Chara* membrane. *Adv. Biophys.* **3**:199–226

Kishimoto, U., Kami-ike, N., Takeuchi, Y. 1980. The role of electrogenic pump in *Chara corallina*. *J. Membrane Biol.* **55**:149–156

Kishimoto, U., Kami-ike, N., Takeuchi, Y. 1981. A quantitative expression of the electrogenic pump and its possible role in the excitation of *Chara* internodes. *In*: The Biophysical Approach to Excitable Systems. W.J. Adelman, Jr., and D.E. Goldman, editors. pp. 165–181. Plenum, New York

Kishimoto, U., Kami-ike, N., Takeuchi, Y., Ohkawa, T. 1984. A kinetic analysis of the electrogenic pump of *Chara corallina*: I. Inhibition of the pump by DCCD. *J. Membrane Biol.* **80**:175–183

Kishimoto, U., Takeuchi, Y., Ohkawa, T., Kami-ike, N. 1985. A kinetic analysis of the electrogenic pump of *Chara corallina*: III. Pump activity during action potential. *J. Membrane Biol.* **86**:27–36

Kitasato, H. 1968. The influence of H^+ on the membrane potential and ion fluxes of *Nitella*. *J. Gen. Physiol.* **52**:60–87

Kotani, P. 1979. A modification of Powell's method for minimization of nonlinear functions. *Computer Center News* (Osaka University) **32**:27–47

Läuger, P. 1979. A channel mechanism for electrogenic ion pumps. *Biochim. Biophys. Acta* **552**:143–161

Läuger, P. 1980. Kinetic properties of ion carriers and channels. *J. Membrane Biol.* **57**:163–178

Oosawa, F., Hayashi, S. 1982. Mechanism of flagellar motor rotation in bacteria. *J. Phys. Soc. Japan* **51**:631–641

Oosawa, F., Hayashi, S. 1984. A loose coupling mechanism of synthesis of ATP by proton flux in the molecular machine of living cells. *J. Phys. Soc. Japan* **53**:1575–1579

Powell, M.J.D. 1965. A method of minimizing a sum of squares

of nonlinear functions without calculating derivatives. *Computer J.* **7**:303–307

Rosing, J., Slater, E.C. 1972. The value of ΔG^o for the hydrolysis of ATP. *Biochim. Biophys. Acta* **267**:275–290

Sanders, D. 1980. The mechanism of Cl^- transport at the plasma membrane of *Chara corallina*. I. Cotransport with H^+. *J. Membrane Biol.* **53**:129–141

Sanders, D., Hansen, U.-P. 1981. Mechanism of Cl^- transport at the plasma membrane of *Chara corallina:* II. Transinhibition and the determination of H^+/Cl^- binding order from a reaction kinetic model. *J. Membrane Biol.* **58**:139–153

Shimmen, T., Tazawa, M. 1977. Control of membrane potential and excitability of *Chara* cells with ATP and Mg^{2+}. *J. Membrane Biol.* **37**:167–192

Shimmen, T., Tazawa, M. 1982. Effects of intracellular vanadate on electrogenesis, excitability and cytoplasmic streaming in *Nitellopsis obtusa*. *Plant Cell Physiol.* **23**:669–677

Spanswick, R.M. 1980. Biophysical control of electrogenecity in the *Characeae*. *In:* Plant Membrane Transport: Current Conceptual Issues. R.M. Spanswick, W.J. Lucas, and J. Dainty. editors. pp. 305–316. Elsevier/North Holland, Amsterdam

Spanswick, R.M. 1981. Electrogenic ion pumps. *Annu. Rev. Plant. Physiol.* **32**:267–289

Takeuchi, Y., Kishimoto, U. 1983. Changes of adenine nucleotide levels in *Chara* internodes during metabolic inhibition. *Plant Cell Physiol.* **24**:1401–1409

Takeuchi, Y., Kishimoto, U., Ohkawa, T., Kami-ike, N. 1985. A kinetic analysis of the electrogenic pump of *Chara corallina:* II. Dependence of the pump on the external pH. *J. Membrane Biol.* **86**:17–26

Received 18 February 1986; revised 3 July 1986

Appendix

The plasmalemma of characean internodes has at least two different ionic pathways, passive and electrogenic. This situation can be most simply and satisfactorily illustrated with the equivalent circuit shown in Fig. A1. The current I in the steady I-V curve, which is actually recorded under the slow-ramp voltage-clamp condition, is the sum of two current components, the one flowing through the passive diffusion channel, i_d, and the other through the electrogenic pump channel, i_p. Then

$$I = i_d + i_p$$
$$i_d = g_d(V\text{-}E_d)$$
$$i_p = g_p(V\text{-}E_p).$$

Therefore,

$$I = G(V\text{-}E)$$
$$G = g_d + g_p$$
$$E = (g_dE_d + g_pE_p)/G.$$

The voltage at which I is zero in the I-V curve is the resting potential E of the membrane. E is the weighted average of two emf's, i.e., E_d and E_p, weights being the conductances of each channel, i.e., g_d and g_p. At the resting potential, the pump current i_p (= $g_p(E\text{-}E_p)$) flows back through the passive channel, causing hyperpolarization of the membrane. The extent of this hyperpolarization, which is equal to i_p/g_d, can be an index of the activity of the electrogenic pump.

If the activity of the electrogenic pump is stopped successfully without affecting the passive diffusion channel, g_p and i_p will decrease to almost zero. Then the I-V curve will converge into the i_d-V curve of the passive diffusion channel. This situation can be realized approximately by treating the *Chara* membrane either with DCCD (dicyclohexylcarbodiimide) or TPC (triphenyltin chloride). Since the i_d-V curve is known, the i_p-V curve of the electrogenic pump can be obtained by simple subtraction of the i_d-V curve from the I-V curve, as long as no qualitative change occurs during each I-V span.

The i_p-V curve thus obtained is sigmoidal in general. It has a reversal potential (E_p) and i_p saturates both with a large depolarization and with a large hyperpolarization. In order to discuss such a nonlinear voltage dependence of the pump characteristics we need to rely on kinetic analysis. Several kinetic models assuming cyclic changes of the enzyme intermediates have been proposed (Läuger, 1979, 1980; Hansen et al., 1981; Chapman, Johnson & Kootsey, 1983; Oosawa & Hayashi, 1982, 1984; Kishimoto et al., 1984, 1985; Takeuchi et al., 1985). Several probable chemical reactions may take place during the cycle (Fig. A2*a*). These are coupling with ATP hydrolysis, occlusion of H^+, release of H^+ and translocation of H^+ (Figs. 6 and A2*a*). In our previous reports (Kishimoto et al., 1985; Takeuchi et al., 1985), we assumed that such reactions were not voltage dependent and considered them together as a single step (Fig. A2*b*). This step is expressed with two voltage-independent rate constants, i.e., κ_{21} (forward) and κ_{12} (backward). Furthermore, only a single step, i.e., translocation of H^+, was to be assumed voltage dependent, which was expressed with the two voltage-dependent rate constants k_{12} (forward) and k_{21} (backward):

$$k_{12} = k^o_{12} \exp(zFV/2RT) \quad \text{(A1)}$$
$$k_{21} = k^o_{21} \exp(-zFV/2RT) \quad \text{(A2)}$$

where z is the number of charges which are translocated during this transition. Asymmetry of energy barrier is possible theoretically (Läuger, 1979, 1980; Chapman et al., 1983). However, in the present analysis we assume symmetry of energy barrier since fitting of the i_p-V curve with this assumption has been quite satisfactory under our experimental condition. Furthermore, we assume that z is equal to m (= the number of H^+ ions occluded into or released from the enzyme). Simulation of the experimental i_p-V curve with Eq. (A3) always gave 2 for z under the normal condition as described in the text. Therefore, the stoichiometric ratio for the H^+ pump in the *Chara* membrane is very likely to be $2H^+/1ATP$ under the normal condition.

Another assumption of steady state for this cycle gives an explicit function for the pump current (i_p). That is,

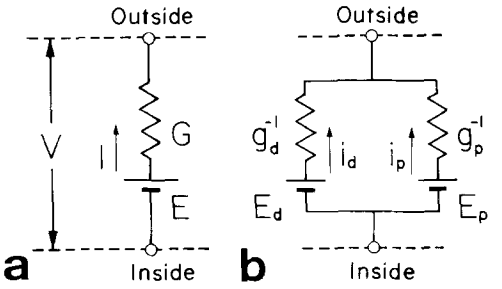

Fig. A1. (*a*) A simplified Thévenin model of the *Chara* membrane. (*b*) Parallel circuit model for the *Chara* membrane having an electrogenic ion pump system in parallel with the passive diffusion channel. The passive diffusion channel as well as the electrogenic pump channel has its own conductance in series with the respective emf

$$i_p = \frac{[\exp(zFV/2RT) - A_1\exp(-zFV/2RT)]\,A_4}{\exp(zFV/2RT) + A_2\exp(-zFV/2RT) + A_3} \tag{A3}$$

where

$$A_1 = (k_{21}^o/k_{12}^o)(\kappa_{12}/\kappa_{21})([\mathrm{ADP}][\mathrm{P_i}]/[\mathrm{ATP}])([\mathrm{H}_o]/[\mathrm{H}_i])^2 \tag{A4}$$

$$A_2 = (k_{21}^o/k_{12}^o) \tag{A5}$$

$$A_3 = (\kappa_{21}[\mathrm{ATP}][\mathrm{H}_i]^2 + \kappa_{12}[\mathrm{ADP}][\mathrm{P_i}][\mathrm{H}_o]^2)/k_{12}^o \tag{A6}$$

$$A_4 = zFE_o\,\kappa_{21}[\mathrm{ATP}][\mathrm{H}_i]^2. \tag{A7}$$

E_o is the density of the H^+-ATPase in the *Chara* plasmalemma. E_o is estimated somewhat arbitrarily to be about $6/(10\ \mu\mathrm{m})^2$, which seems to be a reasonable value as judged by the value of pump conductance. Internal concentrations of ATP, ADP, and P_i are 0.72, 0.35 and 3.0 in mM, respectively (Takeuchi & Kishimoto, 1983). The external pH is 7 and the internal one is assumed to be 7. Four parameters, i.e., A_1, A_2, A_3 and A_4 can be determined by simulating the experimental i_p-V curve with the aid of a computer program of successive approximation by changing each value of parameters independently to find the least sum of squared errors (Powell, 1965: Kotani, 1979).

It is evident from Eq. (A3) that the i_p saturates for a large depolarization at $zFE_o\,\kappa_{21}[\mathrm{ATP}][\mathrm{H}_i]^2$ and for a large hyperpolarization at $-zFE_o\,\kappa_{12}[\mathrm{ADP}][\mathrm{P_i}][\mathrm{H}_o]^2$. The reversal potential (E_p) for the pump is calculated as the voltage where $i_p = 0$.

$$E_p = (RT/2F)\,[\ln(k_{21}^o/k_{12}^o) + \ln(\kappa_{12}/\kappa_{21}) + \ln([\mathrm{ADP}][\mathrm{P_i}]/[\mathrm{ATP}])] + (RT/F)\ln[\mathrm{H}_o]/[\mathrm{H_i}]). \tag{A8}$$

E_p does not depend on voltage, but does to some extent on temperature. The conductance (g_p) of the electrogenic pump is not given as a slope- but as a chord-conductance in our circuit model (Fig. A1).

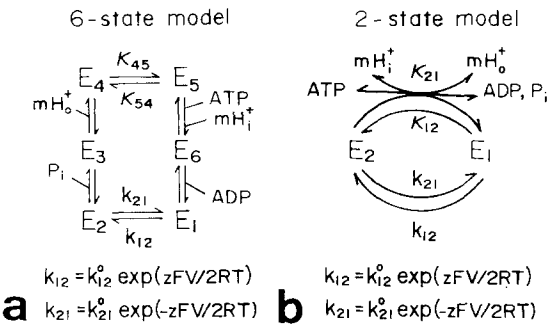

Fig. A2. (*a*) A kinetic scheme for the vectorial H^+-ATPase of the electrogenic pump of the *Chara* membrane. A cyclic change of the H^+-ATPase is assumed. Phosphorylation, dephosphorylation of the enzyme, occlusion of H^+ into and its release from the enzyme, and translocation of H^+ in the enzyme are included in one cycle. The translocation of H^+ in the enzyme occurs during the transition between E_1 and E_2. Only this transition is assumed to be charge carrying and therefore electrogenic. The voltage dependence of this transition is expressed with the voltage-dependent rate constants, k_{12} and k_{21}. (*b*) Nonelectrogenic steps in *a* are lumped together as a single step having voltage-independent rate constants (κ_{21} and κ_{12})

$$g_p = i_p/(V\text{-}E_p). \tag{A9}$$

The g_p depends on the voltage, having a peak at a level somewhat less negative than that of the resting potential. This is plotted with dotted lines in Fig. 2.

The four rate constants can be calculated from Eqs. (A4)-(A7) as follows:

$$\kappa_{21} = A_4/(zFE_o[\mathrm{ATP}][\mathrm{H}_i]^2) \tag{A10}$$

$$\kappa_{12} = A_4(A_1/A_2)/(zFE_o[\mathrm{ADP}][\mathrm{P_i}][\mathrm{H}_o]^2) \tag{A11}$$

$$k_{12}^o = (A_4/A_3)(1 + A_1/A_2)/(zFE_o) \tag{A12}$$

$$k_{21}^o = (A_4/A_3)(A_1 + A_2)/(zFE_o). \tag{A13}$$

Note that the cyclic change of the state of H^+-ATPase of the *Chara* membrane is very fast ($<10^{-6}$ sec; Kishimoto et al., 1985) and the voltage-independent reactions in the cycle are rate limiting, causing saturation of i_p both for a large depolarization and for a large hyperpolarization.